Misorientations in [001] magnetite thin films studied by electron backscatter diffraction and magnetic force microscopy

A. Koblischka-Veneva[a)]
Institute of Functional Materials, University of the Saarland, P.O.Box 151150, Saarbrücken 66041, Germany

M. R. Koblischka and J. D. Wei
Institute of Experimental Physics, University of the Saarland, P.O.Box 151150, Saarbrücken 66041, Germany

Y. Zhou and S. Murphy
SFI Nanoscience Laboratory, Trinity College, Dublin, Dublin 2, Ireland

F. Mücklich
Institute of Functional Materials, University of the Saarland, P.O.Box 151150, Saarbrücken 66041, Germany

U. Hartmann
Institute of Experimental Physics, University of the Saarland, P.O.Box 151150, Saarbrücken 66041, Germany

I. V. Shvets
SFI Nanoscience Laboratory, Trinity College, Dublin, Dublin 2, Ireland

(Presented on 11 January 2007; received 31 October 2006; accepted 20 November 2006; published online 10 April 2007)

Magnetite thin films grown on [001] oriented MgO substrates are analyzed by means of electron backscatter diffraction (EBSD) analysis and magnetic force microscopy in applied fields. The EBSD technique enables the crystallographic orientation of individual grains to be determined with a high spatial resolution up to 20 nm on such ceramic samples. A high image quality of the recorded Kikuchi patterns was achieved enabling multiphase scans and high spatial resolution measurements. Upon annealing in air, the magnetic properties of the magnetite thin films were found to change considerably. Using the EBSD analysis, we find that misoriented grains remaining after the annealing step form small islands with a size of about 100 nm. The size and distribution of these islands correspond well to the observations of antiferromagnetic pinning centers within the magnetic domain structures carried out by magnetic force microscopy on the same samples. © *2007 American Institute of Physics*. [DOI: 10.1063/1.2709424]

I. INTRODUCTION

The observed magnetic properties of magnetite (Fe_3O_4) films are found to be pretty peculiar, as an unexpectedly low efficiency of Fe_3O_4 multilayer spin valves was observed.[1–4] Conversion electron Mössbauer spectroscopy (CEMS) and nuclear resonance data reveal a notable fraction of magnetic moments pointing out of the film plane, while an in-plane orientation would be expected from the interplay of crystalline, magnetoelastic, and shape anisotropies. The films are still unsaturated at 7 T, whereas the magnetization is expected from the anisotropy to be saturated at much lower field values. These unexpected properties appear to be independent of the employed deposition methods and have been related to antiphase boundaries (APBs) existing in epitaxial films.[2,5] For Fe_3O_4 grown on [001] MgO substrates, the lattice constant of the film is twice that of the substrate. As a consequence, stacking faults in the cation sublattice are resulting by forming the APBs. In particular, across some types of APBs, a strong antiferromagnetic coupling is expected. Therefore, a thorough crystallographic analysis of the grain orientations within the magnetite films is required; preferably with a spatial resolution comparable to that of magnetic force microscopy (MFM) measurements. Such an analysis can be provided by the electron backscatter diffraction (EBSD) technique, where with the recent developments a spatial resolution of about 20 nm can be achieved even on oxidic materials.[6–8] Therefore, in this contribution we compare the results of an EBSD orientation analysis with MFM domain patterns on a shortly annealed (1 min in air at 250 °C) magnetite film grown on a [001] MgO substrate.

II. EXPERIMENTAL DETAILS

Epitaxial magnetite thin films with a thickness of 100 nm were grown on MgO single-crystal substrates cut along the [100] direction within ±0.1° by oxygen-plasma-assisted molecular beam epitaxy. Details about the preparation and the *in situ* reflected high energy electron diffraction (RHEED) analysis can be found in Refs. 9 and 10. The film thickness was controlled by quartz-crystal thickness monitors calibrated using x-ray reflectivity. The samples were

[a)]Electronic mail: a.koblischka-veneva@mx.uni-saarland.de

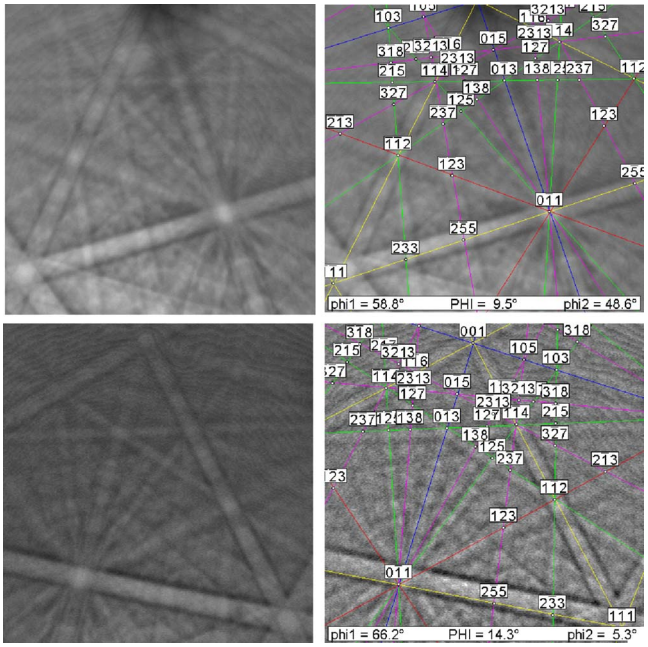

FIG. 1. Kikuchi pattern and the corresponding indexation of magnetite.

subsequently annealed in air at 250 °C; for the present study the duration of annealing was chosen to be 1 min.

The EBSD system employed here consists of a FEI dual beam workstation (Strata DB 235) equipped with a TSL OIM analysis unit.[11] The Kikuchi patterns are generated at an acceleration voltage of 20 kV, and are recorded by means of a DigiView camera system, allowing a maximum recording speed of the order of 0.05 s/pattern. The time employed in the case of a multiphase scan is much longer, of the order of 0.4 s/pattern, as a higher image quality/confidence index is required. To produce a crystallographic orientation map, the electron beam is scanned over a selected surface area and the resulting Kikuchi patterns are indexed and analyzed automatically (i.e., the Kikuchi bands are detected by means of the software). An image quality (IQ) parameter and a confidence index (CI) are recorded for each such Kikuchi pattern. Based on the analysis of the recorded CI value, a multiphase analysis is realized. A detailed description of the measurement procedure can be found in Refs. 12 and 13. The results of the EBSD measurement are presented in form of maps, the most important thereof are the so-called inverse pole figure (IPF) maps, indicating the crystallographic orientation of each individual point. Automated EBSD scans were performed with a step size of 40 nm.

Focused ion beam (FIB) milling was employed to create a set of markers within the magnetite film, so that the exact area can be refound in the subsequent MFM measuresements. In total, five such 20×20 μm^2 big sections were marked by cutting L-shaped markers (1 μm edge length) into the magnetite film. The dose for the FIB milling was kept low at 0.03 nC μm^{-2} in order to ensure no significant damage caused by the ion milling.

Commercial Si cantilevers with 30 nm CoCr magnetic coating were employed for MFM measurements. From imaging of reference samples, these tips were known to be sensitive to the out-of-plane component of the magnetic stray field of the sample. The lift height was in all cases 50 nm.

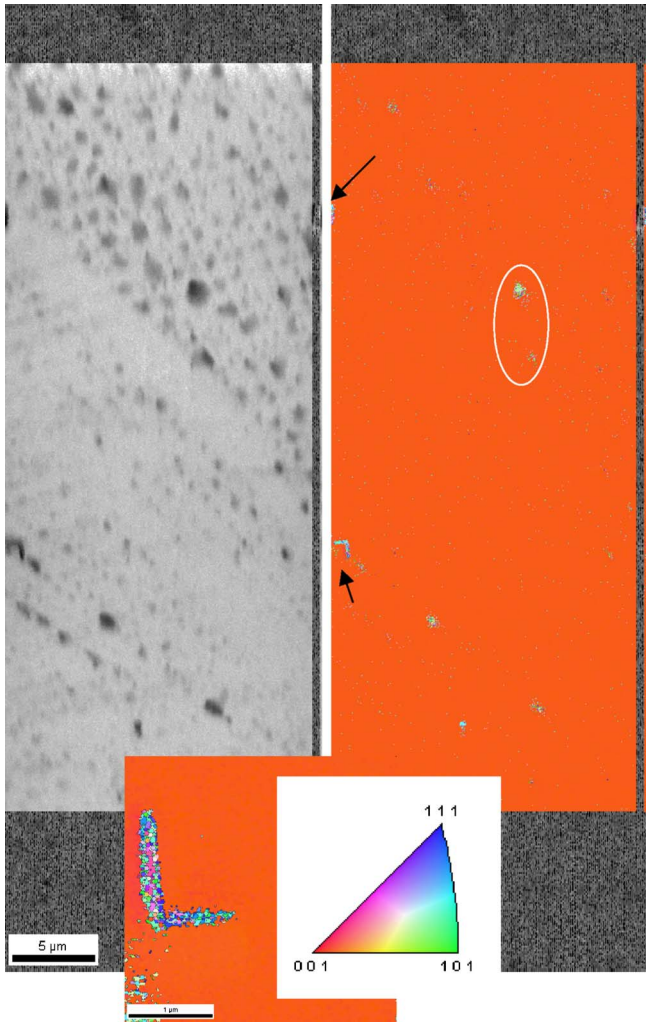

FIG. 2. EBSD analysis of magnetite. The left map is an IQ map and the right one an IPF map, giving the crystallographic orientation. Both maps are put together with an underlying scanning electron microscopy (SEM) image. The color code for the IPF map is given in the stereographic triangle at the bottom. Two L-shaped markers created by FIB milling are marked by arrows. The circle denotes an area with a 30° misorientation embedded in the magnetite matrix. The lower inset gives an orientation analysis around such an L-shaped marker. The edge length of the marker is 1 μm.

III. RESULTS AND DISCUSSION

Figure 1 shows the measured Kikuchi patterns of magnetite together with the indexation by the EBSD system. The determined Eulerian angles are $\varphi_1=66.2°$, $\Phi=14.3°$, and $\varphi_2=5.3°$ for the first pattern and $\varphi_1=58.8°$, $\Phi=9.5°$, and $\varphi_2=48.6°$ for the second one. The IQ achieved is about 300, which is very high for an oxidic ceramic sample, thus enabling automated multiphase scans and high resolution measurements. As compared to the earlier EBSD analysis by Tepper *et al.*,[14] the IQ values recorded here are considerably higher. The Kikuchi patterns clearly reveal the differences between magnetite and maghemite (γ-Fe_2O_3); however, in this paper we do not discuss the differences between these

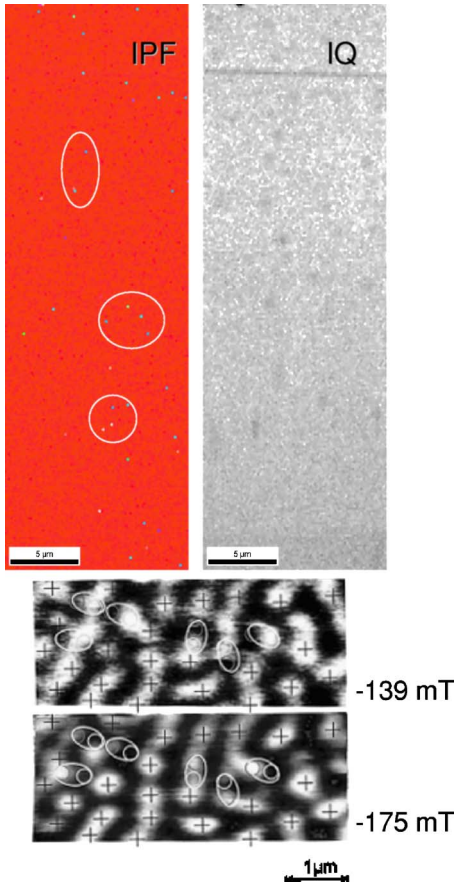

FIG. 3. IPF and IQ maps of an area in between such markers, together with two MFM images taken in the same region. Within the IPF map, several misoriented islands are marked by circles. Their size and distribution correspond well to the specific sites changing polarity in applied fields as indicated in the MFM images. The MFM images are taken at two applied fields, −139 and −175 mT, respectively.

tow components upon annealing. The determined CI value for the magnetite Kikuchi pattern shown is 1, i.e., a perfect indexation.

The changes of microstructure induced by the annealing step in air were discussed in detail in Ref. 7. Here, we focus on the resulting microstructure after the 1 min annealing step, i.e., after that the largest changes of the magnetic properties were observed. Figure 2 presents an EBSD analysis of an area marked by FIB milling (L-shaped patterns as marked by arrows). The left map is an IQ map, while the right map gives the determined crystallographic orientations in an inverse pole figure (IPF) map normal to the sample surface. The applied EBSD stepsize is 40 nm for all maps shown here. The IQ map reveals some structure in the film, which does, however, not play a role in the IPF map. The color code for the IPF map is given in the stereographic triangle. The main orientation of the magnetite film is [001], but characteristically, many small islands with misorientations larger than 30° (green, blue areas) are embedded within the magnetite film; some bigger ones are marked by a circle. The lower inset gives a detail orientation determination of a FIB-produced L-shaped marker. The ion bombardment has created large angle misorientations, which are, however, concentrated on the marker itself. This observation indicates that the ion bombardment to create the markers does not influence the orientation measurements in the selected areas.

Figure 3 presents a comparison of EBSD orientation data with a MFM image taken in the same area of the magnetite film. The EBSD maps are an IPF map (left) and an IQ map (right). The IPF map reveals several misoriented islands with a misorientation above 30°; several of them are marked by circles. These areas are, however, not visible in the IQ map. The MFM images are taken in applied fields of −139 mT (top) and −175 mT (bottom). Details about the MFM measurements can be found in Ref. 15. The areas marked by circles indicate spots which change polarity in this field range. These spots are discussed to be pinning sites for the magnetic domains. From the comparison with the EBSD measurements, it is obvious that the size and distribution of these sites coincide well with the misoriented regions seen by EBSD. The misorientation of more than 30° also creates a different form of magnetic coupling between the islands and the remainder of the magnetite matrix. This will have to be investigated in detail.

The present comparison of EBSD and MFM data obtained on magnetite thin films reveals clearly the importance of a thorough crystallographic analysis of the films in order to understand the magnetic domain patterns measured by means of MFM or other magnetic imaging techniques.

ACKNOWLEDGMENTS

This work is supported by DFG project MU959/19 and the EU-funded project "ASPRINT," which is gratefully acknowledged.

[1] D. T. Margulies, F. T. Parker, M. L. Rudee, F. E. Spada, J. N. Chapman, P. R. Aitchison, and A. E. Berkowitz, Phys. Rev. Lett. **79**, 5162 (1997).
[2] D. T. Margulies, F. T. Parker, F. E. Spada, R. S. Goldman, J. Li, R. Sinclair, and A. E. Berkowitz, Phys. Rev. B **53**, 9175 (1996).
[3] M. Ziese and H. J. Blythe, J. Phys.: Condens. Matter **12**, 13 (2000).
[4] W. L. Zhou, K.-Y. Wang, C. J. O'Conner, and J. Tang, J. Appl. Phys. **89**, 7398 (2001).
[5] S. Celotto, W. Eerenstein, and T. Hibma, Eur. Phys. J. B **36**, 271 (2003).
[6] K. Z. Baba-Kishi, J. Mater. Sci. **37**, 1715 (2002).
[7] A. Koblischka-Veneva, M. R. Koblischka, F. Mücklich, S. Murphy, Y. Zhou, and I. V. Shvets, IEEE Trans. Magn. **42**, 2873 (2006).
[8] A. Koblischka-Veneva, M. R. Koblischka, N. Hari Babu, D. A. Cardwell, L. Shlyk, and G. Krabbes, Supercond. Sci. Technol. **19**, S567 (2006).
[9] Y. Zhou, X. Jin, and I. V. Shvets, J. Appl. Phys. **95**, 7357 (2004).
[10] Y. Zhou, X. Jin, and I. V. Shvets, J. Magn. Magn. Mater. **286**, 346 (2005).
[11] *Orientation Imaging Microscopy software version V4.0, user manual* (TSL, Draper, UT, 2004).
[12] M. R. Koblischka and A. Koblischka-Veneva, Physica C **392–396**, 545 (2003).
[13] A. Koblischka-Veneva, M. R. Koblischka, F. Mücklich, N. Hari Babu, and D. A. Cardwell, Physica C **426–431**, 618 (2005).
[14] T. Tepper, C. A. Ross, and G. F. Dionne, IEEE Trans. Magn. **40**, 1682 (2004).
[15] J. D. Wei, I. Knittel, Y. Zhou, S. Murphy, F. T. Parker, I. V. Shvets, and U. Hartmann, Appl. Phys. Lett. **89**, 122517 (2006).